Progress In Electromagnetics Research, Vol. 105, 213–229, 2010

MODAL ANALYSIS OF MULTILAYER CONICAL DIELECTRIC WAVEGUIDES FOR AZIMUTHAL INVARIANT MODES

A. S. Noor Amin, M. Mirhosseini, and M. Shahabadi

Photonics Research Laboratory
Center of Excellence on Applied Electromagnetics Systems
School of Electrical and Computer Engineering
University of Tehran
North Kargar Ave., Tehran, Iran

Abstract—By using field expansion in terms of the Legendre polynomials and Schelkunoff functions, Maxwell's equations in the spherical coordinate system are cast into a matrix form which lends itself to the analysis of a multilayer conical waveguide. The matrix formulation is then used to obtain an eigen-value problem whose eigen-values are the allowable wave-numbers for propagation in the radial direction. To verify the proposed numerical approach, it is used to evaluate the resonance frequency of a partially filled spherical resonator. The computed resonance frequencies are then compared with those obtained using commercial software based on the finite-element method. The computation time is enormously reduced using the semi-analytical method of this work. Although results are shown for lossless isotropic dielectrics, the method is also applicable to conical waveguides made of lossy dielectrics even with negative permittivity.

1. INTRODUCTION

Tapered optical fibers have found their applications in interconnecting optical waveguide components with different modal spot sizes [1]. This type of conical dielectric waveguides are also utilized in optical couplers [2], filters [3], and near field probes [4]. Obviously, tapered optical metallic waveguides can also be considered as a kind of conical dielectric waveguides. Super-focusing of surface plasmon polaritons (SPPs) as a technique of coupling electromagnetic radiation

Corresponding author: A. S. Noor Amin (a.nooramin@ece.ut.ac.ir).

into a nanoscale structure is made possible with the help of such tapered waveguides. It is well known that super-focusing has many applications such as high-resolution near-field optical microscopy [5], nanolithography [6, 7], plasmonic sensors, and giant surface-enhanced Raman scattering [8–10].

To characterize conical dielectric waveguides, a number of numerical methods have been proposed recently. Stepwise approximation [11, 12], local coupled modes [13], and eikonal approximation [14] are among numerical methods of analysis in the cylindrical coordinate system while the other methods such as finite-difference time-domain (FDTD) [15, 16], quasi-separation of variables approach [17, 18], beam propagation method (BPM) [3], finite-difference beam propagation method [4] and finite-element method (FEM) [19] are proposed in the spherical coordinate system.

The goal of this work is introduction of a semi-analytical modal analysis for multilayer conical dielectric waveguides in the spherical coordinate system. Using the Legendre polynomials and the Schelkunoff functions as a complete orthogonal basis to expand the fields, we arrive at a matrix representation of Maxwell's equations in terms of non-radial field components. In the following sections, we have derived the mathematical relations that generally govern the spatial variation of space harmonics propagating in conical multilayer dielectric waveguides. The steps toward obtaining the required equations for any given dielectric conical waveguides are straightforwards and systematic, which renders the method versatile.

2. FORMULATION

In Figure 1, a typical multilayer conical waveguide is depicted. We employ a spherical system of coordinates (r, θ, φ) for this geometry. This tapered waveguide is composed of linear homogeneous isotropic non-magnetic dielectrics whose permittivity is independent of r and φ.

The relative permittivity of the tapered waveguide is assumed to be a step function of θ as shown in Figure 2. Here, the relative permittivity of the region $\alpha_n < \theta < \alpha_{n+1}$ is the complex value $\varepsilon_{r_{n+1}}$. We seek to present a general form of the solution to Maxwell's equations in this configuration.

The dielectric constant or $\varepsilon_r(\theta)$ can be uniquely expanded in terms of the Legendre polynomials which form a complete set of orthogonal basis functions over $0 \leq \theta \leq \pi$. One may then write

$$\varepsilon_r(\theta) = \lim_{M \to \infty} \sum_{m=0}^{M} c_m P_m(\cos\theta) \tag{1}$$

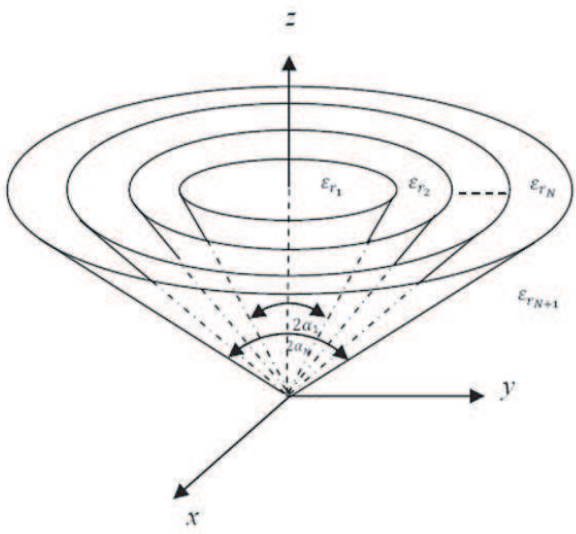

Figure 1. Typical multilayer conical dielectric waveguide.

where $P_m(\cos\theta)$ are the Legendre polynomials of the first kind and the m-th order. Values of the coefficients c_m are given by

$$c_m = \frac{2m+1}{2} \int_0^{\pi} \varepsilon_r(\theta) P_m(\cos\theta) \sin\theta d\theta \tag{2}$$

In this work, only φ-invariant electromagnetic fields are taken into

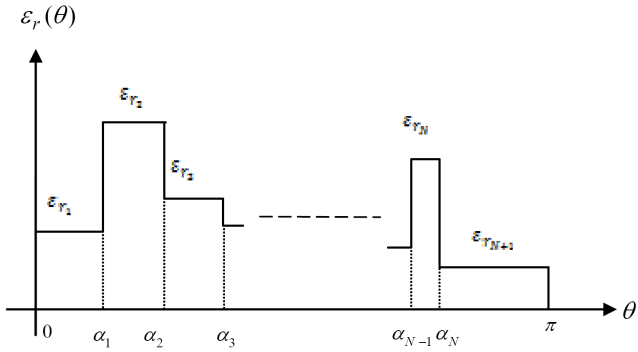

Figure 2. Relative permittivity profile of a multilayer conical dielectric waveguide.

consideration. In the following subsection, we first obtain a general form of solution.

2.1. General Form of Solution

In a spherical system of coordinates, every electromagnetic field distribution can be expressed in terms of a linear combination of a TM to r (TM_r) and a TE to r (TE_r) electromagnetic field [20]. For TM_r waves, a vector potential $\vec{A} = A^r(r,\theta)\hat{r}$ is chosen such that $\vec{H} = \nabla \times \vec{A}$. We assume $\exp(i\omega t)$ for time variation of the electromagnetic field. From Maxwell's equation, one can show that $\vec{A}$ satisfies

$$\nabla\left(\frac{1}{\varepsilon_r(\theta)}\right)\times\left(\nabla\times\left(\nabla\times\vec{A}\right)\right)+\frac{1}{\varepsilon_r(\theta)}\nabla\times\left(\nabla\times\left(\nabla\times\vec{A}\right)\right)-k_0^2\nabla\times\vec{A}=0 \quad (3)$$

for the configuration of Figure 1 where $\varepsilon_r(\theta)$ denotes the θ-dependent relative permittivity and $k_0^2 = \omega^2\mu_0\varepsilon_0$. Applying the method of separation of variables, we suggest

$$A^r(r,\theta) = R(r)\,T(\theta) \quad (4)$$

as a solution to (3). Substituting (4) in (3), we arrive at

$$\begin{aligned}
&\frac{r^2\left(\frac{d^2}{dr^2}R(r)\right)}{R(r)}+k_0^2\varepsilon_r(\theta)r^2\\
&=-\frac{\varepsilon_r(\theta)\sin^2\theta\left(\frac{d^3}{d\theta^3}T(\theta)\right)+\sin\theta\cos\theta\left(\frac{d}{d\theta}\varepsilon_r(\theta)\right)\left(\frac{d}{d\theta}T(\theta)\right)}{\varepsilon_r(\theta)\sin^2\theta\left(\frac{d}{d\theta}T(\theta)\right)}\\
&+\frac{\varepsilon_r(\theta)\left(\frac{d}{d\theta}T(\theta)\right)-\varepsilon_r(\theta)\cos\theta\sin\theta\left(\frac{d^2}{d\theta^2}T(\theta)\right)+\sin^2\theta\left(\frac{d}{d\theta}\varepsilon_r(\theta)\right)\left(\frac{d^2}{d\theta^2}T(\theta)\right)}{\varepsilon_r(\theta)\sin^2\theta\left(\frac{d}{d\theta}T(\theta)\right)} \quad (5)
\end{aligned}$$

Similar to $\varepsilon_r(\theta)$, an expression in terms of the Legendre polynomials is used to expand $T(\theta)$, i.e.,

$$T(\theta) = \lim_{N\to\infty}\sum_{n=0}^{N} a_n P_n(\cos\theta) \quad (6)$$

Since $P_n(\cos\theta)$ satisfies the Legendre differential equation, substituting (6) in (5) will result in

$$\begin{aligned}
&\left(\frac{d^2}{dr^2}R(r)+k_0^2\varepsilon_r(\theta)R(r)\right)\varepsilon_r(\theta)\sin^2\theta\sum_{n=0}^{N}a_n\frac{d}{d\theta}P_n(\cos\theta)\\
&=\ -\frac{R(r)}{r^2}\frac{d}{d\theta}\sum_{n=0}^{N}n(n+1)a_n\varepsilon_r(\theta)P_n(\cos\theta) \quad (7)
\end{aligned}$$

Replacing $\varepsilon_r(\theta)$ in (7) by the expansion given by (1) yields

$$\begin{aligned}
&\frac{d^2}{dr^2}R(r)\sum_{n=0}^{N}\sum_{m=0}^{M}a_nc_m\sin^2\theta P_n(\cos\theta)\frac{d}{d\theta}P_m(\cos\theta)\\
&+k_0^2R(r)\sum_{n=0}^{N}\sum_{m=0}^{M}\sum_{l=0}^{N}a_nc_lc_m\sin^2\theta P_m(\cos\theta)P_l(\cos\theta)\frac{d}{d\theta}P_n(\cos\theta)\\
=\;&-\frac{R(r)}{r^2}\frac{d}{d\theta}\sum_{n=0}^{N}\sum_{m=0}^{M}n(n+1)a_nc_mP_n(\cos\theta)P_m(\cos\theta) \qquad (8)
\end{aligned}$$

As will be shown later, both $P_n(\cos\theta)P_m(\cos\theta)$ and $\frac{d}{d\theta}P_n(\cos\theta)$ appearing in (8) can be expanded in terms of $P_n(\cos\theta)$. Hence, one can reformulate (8) as

$$\sum_{n=0}^{N}\left(\frac{d^2}{dr^2}R(r)U_n+k_0^2R(r)\,V_n+\frac{R(r)}{r^2}W_n\right)P_n(\cos\theta)=0 \qquad (9)$$

where *θ-independent* U_n, V_n, and W_n are functions of a_i, c_j and the remaining expansion coefficients. Since $\{P_n(\cos\theta)\}$ form a complete set of functions, the summation in (9) will be zero if and only if the coefficients are all zero. This leads to a set of *r-dependent* differential equations.

Now, we concentrate on $R(r)$ in (9). We introduce a set of functions $\{\hat{H}_m(kr)\}$ which are all solutions to

$$\frac{d^2}{dr^2}\hat{H}_m(kr)+k^2\hat{H}_m(kr)+\frac{m(m+1)}{r^2}\hat{H}_m(kr)=0 \qquad (10)$$

These functions are known as the Schelkunoff functions and are closely related to the spherical Hankel functions [18]. Here, we try the following expansion for $R(r)$

$$R(r)=\lim_{M\to\infty}\sum_{m=0}^{M}b_m\hat{H}_m(kr) \qquad (11)$$

Substituting (11) in (9) and after some simplifications, we will obtain for $n=0,1,2,\ldots,N$,

$$\begin{aligned}
&\lim_{M\to\infty}\sum_{m=0}^{M}\left[-m(m+1)b_mU_n+b_mW_n\right]\sum_{l=L_{down}(m)}^{L_{up}(m)}\xi_l\hat{H}_l(kr)\\
&+\left(k_0^2b_mV_n-k^2b_mU_n\right)\hat{H}_m(kr)=0 \qquad (12)
\end{aligned}$$

In which we have used the following recursive identity

$$\frac{1}{r^2}\hat{H}_m(kr) = k^2\left(\frac{1}{(2m-1)(2m+1)}\hat{H}_{m-2}(kr) + \frac{2}{(2m-1)(2m+3)}\hat{H}_m(kr) + \frac{2}{(2m+1)(2m+3)}\hat{H}_{m+2}(kr)\right) \quad (13)$$

In (12), the r-independent parameters ξ_l, $L_{down}(m)$, and $L_{up}(m)$ are the coefficients, lower limit and upper limit of the summation, respectively. Since the Schelkunoff functions are orthogonal over $-\infty < r < \infty$ [21], the summation in (12) will be zero if and only if the coefficients are all zero. Thus, a system of equations is obtained in which the propagation constant k as well as the expansion coefficients a_i and b_j can be determined from its eigen-vectors and eigen-values.

As mentioned previously, $\vec{A}$ is assumed to be independent of φ. So, the magnetic field component are calculated as follow [22],

$$\begin{aligned}
\vec{H}\cdot\hat{r} &= (\nabla\times\vec{A})\cdot\hat{r} = \frac{1}{r\sin\theta}\left(\frac{\partial}{\partial\theta}(\sin\theta A^{\varphi}) - \frac{\partial}{\partial\varphi}A^{\theta}\right) = 0\\
\vec{H}\cdot\hat{\theta} &= (\nabla\times\vec{A})\cdot\hat{\theta} = \frac{1}{r\sin\theta}\left(\frac{\partial}{\partial\varphi}A^{r} - \frac{\partial}{\partial r}r\sin\theta A^{\varphi}\right) = 0\\
\vec{H}\cdot\hat{\varphi} &= (\nabla\times\vec{A})\cdot\hat{\varphi} = \frac{1}{r}\left(\frac{\partial}{\partial r}rA^{\theta} - \frac{\partial}{\partial\theta}A^{r}\right) = -\frac{\partial}{r\partial\theta}A^{r}
\end{aligned} \quad (14)$$

As shown in (14), the magnetic field only has a φ-component whose variation as a function of r is $\frac{-1}{r}R(r)$. Similarly, the displacement vector can be determined as follows,

$$\begin{aligned}
\vec{D}\cdot\hat{r} &= \frac{-1}{i\omega}(\nabla\times\vec{H})\cdot\hat{r} = \frac{1}{i\omega r^2\sin\theta}\left(\frac{\partial}{\partial\theta}\left(\sin\theta\frac{\partial}{\partial\theta}A^{r}\right)\right)\\
\vec{D}\cdot\hat{\theta} &= \frac{-1}{i\omega}(\nabla\times\vec{H})\cdot\hat{\theta} = \frac{-1}{i\omega r}\left(\frac{\partial^2}{\partial r\partial\theta}A^{r}\right)\\
\vec{D}\cdot\hat{\varphi} &= \frac{-1}{i\omega}(\nabla\times\vec{H})\cdot\hat{\varphi} = \frac{1}{i\omega r\sin\theta}\left(\frac{\partial^2}{\partial r\partial\varphi}H^{r}\right) = 0
\end{aligned} \quad (15)$$

Since the relative permittivity of the conical dielectric waveguide is assumed to be r-independent, the electric field and the displacement vector behave similarly. So, two non-zero components of the electric field E^{θ} and E^{r} will vary as $\frac{1}{r}\frac{d}{dr}R(r)$ and $\frac{1}{r^2}R(r)$, respectively. Because of the identity

$$\frac{d}{dr}\hat{H}_m(kr) = k\left(\frac{m+1}{2m+1}\hat{H}_{m-1}(kr) - \frac{m}{2m+1}\hat{H}_{m+1}(kr)\right) \quad (16)$$

and (13), it is obvious that H^{φ} and E^{θ} or the transverse (non-radial) field components are related to $\frac{1}{r}\hat{H}_m(kr)$ while E^r or the radial component is proportional to $\hat{H}_m(kr)$. A similar discussion is also true for TE_r waves.

If $\vec{F}$ stands for the electric or the magnetic field vector, then we define $F^u(r,\theta) = \vec{F}(r,\theta) \cdot \hat{u}$ where $\hat{u} \in \left\{\hat{r}, \hat{\theta}, \hat{\varphi}\right\}$. Therefore, the general form of a solution to Maxwell's equations in a conical dielectric waveguide is

$$r^{\gamma} F^u(r,\theta) = \lim_{M,N\to\infty} \sum_{m=0}^{M} \sum_{n=0}^{N} f^u_{m,n} \hat{H}_m(kr) P_n(\cos\theta) \tag{17}$$

$f^u_{m,n}$ are expansion coefficients and k is the propagation constant. In (17), γ equals to 0 or 1 for the radial or transverse (non-radial) components of electromagnetic fields, respectively. It should be mentioned that the method of separation of variables cannot be used directly to obtain the general form of (17) for a multilayer conical dielectric waveguide. This is because the relative permittivity of the waveguide is a function of θ so that the differential equation of (3) cannot be separated in two differential equations for $R(r)$ and $T(\theta)$. On the other hand, it is also impossible to represent a solution for a conical dielectric waveguide by solving Maxwell's equation in each homogenous region of the waveguide and applying boundary conditions to match the fields. This is true because the propagation constant long $\hat{r}$ in the spherical coordinate system only depends on the medium characteristic. Hence, it has different values in each homogeneous region of the waveguide and obviously the boundary conditions at $\theta = \alpha_n$ of Figure 1 cannot be satisfied.

Determination of the propagation constant k of a mode and its corresponding mode field by solving the system of equations obtained from (12) are cumbersome. Instead, by applying the matrix representation of Maxwell's equation and using the general form of a solution (17), it is shown shortly that $f^u_{m,n}$ satisfy an eigen-value problem whose eigen-values are allowable values of k. To derive this system of equations use is made of matrix algebra, as summarized in the following sub-sections.

2.2. Matrix Representation

We define a single-column matrix $[f^u]$ the entries of which are $f^u_{m,n}$. From (17), it is obvious that $[f^u]$ must possess $K = (M+1) \times (N+1)$ rows to accommodate all $f^u_{m,n}$. The coefficients $f^u_{m,n}$ are sorted by

letting the indices m and n assume integer values according to

$$[m_1, m_2, \ldots, m_K] = [0, 1, 2, \ldots, M] \otimes [\underbrace{1, 1, \ldots, 1}_{N+1}] \tag{18}$$

and

$$[n_1, n_2, \ldots, n_K] = [\underbrace{1, 1, \ldots, 1}_{M+1}] \otimes [0, 1, 2, \ldots, N], \tag{19}$$

respectively, where $\otimes$ denotes the Kronecker tensor product of the matrices $\mathbb{A}$ and $\mathbb{B}$, which is defined as

$$\mathbb{A} \otimes \mathbb{B} = \begin{bmatrix} a_{11} & a_{12} & \cdots \\ a_{21} & a_{22} & \cdots \\ \vdots & \vdots & \ddots \end{bmatrix} \otimes \mathbb{B} = \begin{bmatrix} a_{11}\mathbb{B} & a_{12}\mathbb{B} & \cdots \\ a_{21}\mathbb{B} & a_{22}\mathbb{B} & \cdots \\ \vdots & \vdots & \ddots \end{bmatrix} \tag{20}$$

Similarly, a single-column matrix function $[\mathcal{F}^u(r,\theta)]$ is defined using (17) as follows

$$[\mathcal{F}^u(r,\theta)] = \left[\mathbb{I}_{(M+1)\times(M+1)} \otimes \mathbb{P}(\theta)\right] \left[r^{-\gamma}\mathbb{H}(kr) \otimes \mathbb{I}_{(N+1)\times(N+1)}\right] [f^u] \tag{21}$$

where $\mathbb{P}(\theta)_{j,j} = P_{j-1}(\cos\theta)$, $\mathbb{H}(kr)_{l,l} = \hat{H}_{l-1}(kr)$ for $j = 1, 2, \ldots, N$ and $l = 1, 2, \ldots, M$. Here, $[\mathcal{F}^u(r,\theta)]$ has K rows and $\mathbb{I}$ is an identity matrix. For instance, the entries of $[\mathcal{E}^r(r,\theta)]$ matrix are $e^u_{m,n}\hat{H}_m(kr)P_n(\cos\theta)$ and the entries of $[e^r]$ are $f^u_{m,n}$.

We now turn our attention to the spatial derivative with respect to θ of various field components in the spherical coordinate, for instance $\frac{\partial F^u(r,\theta)}{\sin\theta \partial\theta}$. The equivalent matrix operation for this differentiation is shown in Table 1 which is obtained by the help of the following identity

$$\frac{-1}{\sin\theta}\frac{d}{d\theta}P_n(\cos\theta) = \begin{cases} \sum_{i=1}^{h}(4i-1)P_{2i-1}(\cos\theta) & n = 2h \\ \sum_{i=0}^{h}(4i+1)P_{2i}(\cos\theta) & n = 2h+1 \end{cases} \tag{22}$$

which we have derived by the method of induction. Similarly, the identity

$$\cos\theta P_n(\cos\theta) = \frac{n}{2n+1}P_{n-1}(\cos\theta) + \frac{n+1}{2n+1}P_{n+1}(\cos\theta) \tag{23}$$

is used to determine the coefficients for expansion of $\cos\theta F^u(r,\theta)$ in terms of the Legendre polynomials. Applying (23), the matrix operation equivalent to $\cos\theta F^u(r,\theta)$ is obtained and shown in Table 1. As we show later, applying (22) and (23) is necessary to simplify the matrix representation of Maxwell's equations.

Table 1. Matrix operations equivalent to commonly appearing operations on $F^u(r,\theta)$.

Operation on $F^u(r,\theta)$	Equivalent matrix operation
$\frac{-1}{\sin\theta}\frac{\partial}{\partial\theta}F^u(r,\theta)$	$\left[\mathbb{I}_{(M+1)\times(M+1)}\otimes\mathbb{P}(\theta)\right]$ $\left[r^{-\gamma}\mathbb{H}(kr)\otimes\mathbb{I}_{(N+1)\times(N+1)}\right]$ $\left[\mathbb{I}_{(M+1)\times(M+1)}\otimes\mathbb{P}_d\right][f^u]$
$\cos\theta F^u(r,\theta)$	$\left[\mathbb{I}_{(M+1)\times(M+1)}\otimes\mathbb{P}(\theta)\right]$ $\left[r^{-\gamma}\mathbb{H}(kr)\otimes\mathbb{I}_{(N+1)\times(N+1)}\right]$ $\left[\mathbb{I}_{(M+1)\times(M+1)}\otimes\mathbb{P}_{\cos}\right][f^u]$
where $\mathbb{P}_{d_{m,n}}=\begin{cases}4l-3 & m=2l-1, n=2j+2\\ 4l-1 & m=2l, n=2j+3\end{cases}$ $\quad$ $\mathbb{P}_{\cos_{m,n}}=\begin{cases}\frac{l}{2l+1} & m=l, n=l+1\\ \frac{l}{2l-1} & m=l, n=l-1\end{cases}$ $l=1,2,\ldots,M+1, j=l-1,l,l+1,\ldots,\frac{M-1}{2}$	

2.3. Constitutive Relations

Presenting an equivalent matrix expression for the constitutive relations is the goal of this section. The constitutive relations in the spatial domain are as follows

$$D^u(r,\theta)=\varepsilon_0\varepsilon_r(\theta)E^u(r,\theta) \tag{24}$$

and

$$B^u(r,\theta)=\mu_0 H^u(r,\theta). \tag{25}$$

By using (17) and (24), we can write

$$\begin{aligned}D^u(r,\theta)&=\varepsilon_0\lim_{L\to\infty}\sum_{l=0}^{L}c_l P_l(\cos\theta)\lim_{M,N\to\infty}\sum_{n=0}^{N}\sum_{m=0}^{M}e^u_{m,n}P_n(\cos\theta)\hat{H}_m(kr)\\&=\varepsilon_0\lim_{M,N,L\to\infty}\sum_{l=0}^{L}\sum_{m=0}^{M}\sum_{n=0}^{N}c_l e^u_{m,n}P_l(\cos\theta)P_n(\cos\theta)\hat{H}_m(kr)\end{aligned} \tag{26}$$

where $e^u_{m,n}$ are electric field coefficients to be calculated later. To cast (26) in the form of (17), it is necessary to replace $P_l(\cos\theta)P_n(\cos\theta)$ by a summation in terms of $P_n(\cos\theta)$. We have derived the following identity

$$P_n(\cos\theta)P_m(\cos\theta)=\sum_{h=0}^{m}\varsigma(h,n,m)P_{n+m-2h}(\cos\theta)\quad(n\geq m) \tag{27}$$

where

$$\varsigma(h,n,m) = \frac{\prod_{j=1-h}^{m-h}(n+j)}{\prod_{l=-h}^{m-2h-1}(2n+2l+1)\prod_{i=m-2h+1}^{m-h}(2n+2i+1)} \left(\frac{(2(m-h))!}{2^{m-h}((m-h)!)^2}\right)\left(\frac{(2h)!}{2^h(h!)^2}\right). \tag{28}$$

(28) is also derived in [23]; however, the above form is a compact closed form. Substitution of (27) in (26) yields

$$D^u(r,\theta) = \varepsilon_0 \lim_{M,N\to\infty} \sum_{n=0}^{N}\sum_{m=0}^{M} d^u_{m,n} P_n(\cos\theta)\hat{H}_m(kr) \tag{29}$$

where

$$d^u_{m,2l} = \sum_{s=0}^{\infty} \begin{cases} \sum_{h_n=\mathrm{Max}(l-h_s,0)}^{h_s+l} c_s e^u_{m,2h_n}\varsigma(h_n+h_s-l,2h_n,2h_s) & s=2h_s \\ \sum_{h_n=\mathrm{Max}(l-h_s-1,0)}^{h_s+l} c_s e^u_{m,2h_n+1}\varsigma(h_n+h_s-l+1,2h_n+1,2h_s+1) & s=2h_s+1 \end{cases}$$

$$d^u_{m,2l+1} = \sum_{s=0}^{\infty} \begin{cases} \sum_{h_n=\mathrm{Max}(l-h_s,0)}^{h_s+l} c_s e^u_{m,2h_n+1}\varsigma(h_n+h_s-l,2h_n+1,2h_s) & s=2h_s \\ \sum_{h_n=\mathrm{Max}(l-h_s,0)}^{h_s+l+1} c_s e^u_{m,2h_n}\varsigma(h_n+h_s-l,2h_n,2h_s+1) & s=2h_s+1 \end{cases}$$

$l=0,\ 1,\ 2,\ldots$ (30)

With the help of (30), the desired expansion coefficients of (29) can be calculated. Since (29) is in the form of (17), it can be represented in a matrix form. So, we define three single-column matrices $[f^u]$ which accommodate the expansion coefficients of $D^u(r,\theta)$. Note that again we sort these coefficients according to the index pairs given by (18) and (19). Using these matrices and after some algebraic manipulations, we obtain

$$[d^u] = \varepsilon_0 \mathbb{N}^2 [e^u] \tag{31}$$

Here, the matrix $\mathbb{N}^2$ has K rows and K columns and is comprised of $(M+1)\times(M+1)$ sub-matrices as follows

$$\mathbb{N}^2 = \mathbb{I}_{(M+1)\times(M+1)} \otimes \mathbb{N}'^2 \tag{32}$$

In which the entries of the sub-matrix $\mathbb{N}'^2$ are determined with the help of (30).

2.4. Matrix Formulation of Maxwell's Equations

Using the matrices introduced in the previous sections, we are now able to derive the desired formulations. For this purpose, the proposed solution given by (17) along with the constitutive relations (24) and (25) are substituted in Maxwell's equations. Elimination of the $[\mathcal{E}^r(r,\theta)]$ and $[\mathcal{H}^r(r,\theta)]$ in the matrix representation of Maxwell's equations, and reformulating it based on $[\mathcal{E}^\varphi(r,\theta)]$ and $[\mathcal{H}^\varphi(r,\theta)]$, we will achieve to

$$\begin{aligned}
&\left\{ \frac{d^2}{dr^2} \left[\mathbb{H}(kr) \otimes \mathbb{I}_{(N+1)\times(N+1)}\right] \left[\mathbb{I}_{(M+1)\times(M+1)} \otimes \mathbb{P}_{\sin^2}\right] \right. \\
&+\omega^2\mu_0\varepsilon_0 \left[\mathbb{H}(kr) \otimes \mathbb{I}_{(N+1)\times(N+1)}\right] \left[\mathbb{I}_{(M+1)\times(M+1)} \otimes \mathbb{P}_{\sin^2}\right] \mathbb{N}^2 \\
&-\frac{1}{r^2} \left[\mathbb{H}(kr) \otimes \mathbb{I}_{(N+1)\times(N+1)}\right] \\
&\left.\left[\mathbb{I}_{(M+1)\times(M+1)} \otimes \left[\mathbb{I}_{(N+1)\times(N+1)} - \mathbb{P}_{d\sin}\mathbb{P}_{\cos} - \mathbb{P}_{\sin^2}\mathbb{P}_{d^2}\right]\right] \right\} [e^\varphi] = 0 \quad (33) \\
&\left\{ \frac{d^2}{dr^2} \left[\mathbb{H}(kr) \otimes \mathbb{I}_{(N+1)\times(N+1)}\right] \left[\mathbb{I}_{(M+1)\times(M+1)} \otimes \mathbb{P}_{\sin^2}\right] \mathbb{N}^{-2} \right. \\
&+\omega^2\mu_0\varepsilon_0 \left[\mathbb{H}(kr) \otimes \mathbb{I}_{(N+1)\times(N+1)}\right] \left[\mathbb{I}_{(M+1)\times(M+1)} \otimes \mathbb{P}_{\sin^2}\right] \\
&\frac{1}{r^2} \left[\mathbb{H}(kr) \otimes \mathbb{I}_{(N+1)\times(N+1)}\right] \left[\mathbb{I}_{(M+1)\times(M+1)} \otimes \left(-\mathbb{P}_{\cos} + \mathbb{P}_{d\sin}\right)\right] \\
&\left.+ \mathbb{N}^{-2} \left[\mathbb{I}_{(M+1)\times(M+1)} \otimes \left(\mathbb{P}_{\cos} + \mathbb{P}_{d\sin}\right)\right] \right\} [h^\varphi] = 0 \quad (34)
\end{aligned}$$

where $\mathbb{P}_{\sin^2} = \mathbb{I}_{(N+1)\times(N+1)} - \mathbb{P}^2_{\cos}$, $\mathbb{P}_{d\sin} = -\mathbb{P}_{\sin^2}\mathbb{P}_d$, and $\mathbb{P}_{d^2} = -\mathbb{P}_{\cos}\mathbb{P}_d + \mathbb{P}_{\sin^2}\mathbb{P}^2_d$.

As mentioned previously, the Schelkunoff functions are solutions to the differential equations (33) and (34). So, $\hat{H}^{(1)}_m(kr)$ or $\hat{H}^{(2)}_m(kr)$ can be employed for incoming and outgoing traveling waves along $\hat{r}$, respectively. Here, k is the mode propagation constant which will be determined later.

Now, we turn our attentions to the spatial derivative of various field components with respect to r. With the help of (16), matrix equivalent of $\frac{\partial}{\partial r}F^u(r,\theta)$ can be represented as shown in Table 2. Also, the matrix equivalent to $\frac{1}{r^2}F^u(r,\theta)$ is given in Table 2 which is calculated by the help of (13). After applying the relations of Table 2 and after some algebraic manipulations, we arrive at the following

Table 2. Matrix operations equivalent to commonly appearing operations for non-radial components on $F^u(r,\theta)$.

Operation on $F^u(r,\theta)$	Equivalent matrix operation
$\frac{1}{r^2}F^u(r,\theta)$	$k^2\left[\mathbb{I}_{(M+1)\times(M+1)}\otimes\mathbb{P}(\theta)\right]$ $\left[\mathbb{H}(kr)\otimes\mathbb{I}_{(N+1)\times(N+1)}\right]$ $\left[\mathbb{H}_{\frac{1}{r^2}}\otimes\mathbb{I}_{(N+1)\times(N+1)}\right][f^u]$
$\frac{\partial}{\partial r}F^u(r,\theta)$	$k\left[\mathbb{I}_{(M+1)\times(M+1)}\otimes\mathbb{P}(\theta)\right]$ $\left[\mathbb{H}(kr)\otimes\mathbb{I}_{(N+1)\times(N+1)}\right]$ $\left[\mathbb{H}_d\otimes\mathbb{I}_{(N+1)\times(N+1)}\right][f^u]$
where $\mathbb{H}_{d_{m,n}}=\begin{cases}\delta & m=n=1\\ \frac{l+1}{2l+1} & m=l,n=l+1\\ \frac{2-l}{2l-3} & m=l,n=l-1\end{cases}$	$\mathbb{H}_{\frac{1}{r^2}{}_{m,n}}=\begin{cases}\delta & m=1,n=2\\ \frac{\delta}{3} & m=2,n=1\\ \frac{1}{(2l-3)(2l-5)} & m=l,n=l-2\\ \frac{2}{(2l-3)(2l+1)} & m=n=l\\ \frac{1}{(2l+1)(2l+3)} & m=l,n=l+2\end{cases}$
for $l=1,2,\ldots,N+1$.	
δ equals to $+i$ or $-i$ for corresponding $\hat{H}_m^{(1)}(kr)$ and $\hat{H}_m^{(2)}(kr)$, respectively.	

eigen-equations for $[e^\varphi]$ and $[h^\varphi]$

$$\Big\{k^2\left[\mathbb{H}_d^2\otimes\mathbb{I}_{(N+1)\times(N+1)}\right]\left[\mathbb{I}_{(M+1)\times(M+1)}\otimes\mathbb{P}_{\sin^2}\right]$$
$$+\omega^2\mu_0\varepsilon_0\left[\mathbb{I}_{(M+1)\times(M+1)}\otimes\mathbb{P}_{\sin^2}\right]\mathbb{N}^2-k^2\left[\mathbb{H}_{\frac{1}{r^2}}\otimes\mathbb{I}_{(N+1)\times(N+1)}\right]$$
$$\left[\mathbb{I}_{(M+1)\times(M+1)}\otimes\left[\mathbb{I}_{(N+1)\times(N+1)}-\mathbb{P}_{d\sin}\mathbb{P}_{\cos}-\mathbb{P}_{\sin^2}\mathbb{P}_{d^2}\right]\right]\Big\}[e^\varphi]=0 \quad (35)$$

$$\Big\{k^2\left[\mathbb{H}_d^2\otimes\mathbb{I}_{(N+1)\times(N+1)}\right]\left[\mathbb{I}_{(M+1)\times(M+1)}\otimes\mathbb{P}_{\sin^2}\right]\mathbb{N}^{-2}$$
$$+\omega^2\mu_0\varepsilon_0\left[\mathbb{I}_{(M+1)\times(M+1)}\otimes\mathbb{P}_{\sin^2}\right]$$
$$+k^2\left[\mathbb{H}_{\frac{1}{r^2}}\otimes\mathbb{I}_{(N+1)\times(N+1)}\right]\left[\mathbb{I}_{(M+1)\times(M+1)}\otimes\left(-\mathbb{P}_{\cos}+\mathbb{P}_{d\sin}\right)\right]$$
$$\mathbb{N}^{-2}\left[\mathbb{I}_{(M+1)\times(M+1)}\otimes\left(\mathbb{P}_{\cos}+\mathbb{P}_{d\sin}\right)\right]\Big\}[h^\varphi]=0 \quad (36)$$

By solving (35) and (36), the propagation constant k as well as the complex amplitudes of $[e^\varphi]$ and $[h^\varphi]$ can be achieved. The remaining

two components of the fields can be calculated with the help of

$$[h^{\theta}] = \frac{k}{i\omega\mu_0}\left[\mathbb{H}_d^{\otimes}\mathbb{I}_{(N+1)\times(N+1)}\right][e^{\varphi}] \tag{37}$$

$$[e^{\theta}] = \frac{-k}{i\omega\varepsilon_0}\mathbb{N}^{-2}\left[\mathbb{H}_d^{\otimes}\mathbb{I}_{(N+1)\times(N+1)}\right][h^{\varphi}] \tag{38}$$

In summary, the following steps are to be taken for a full-wave modal analysis of a given conical dielectric waveguide:

Step 1: Construction of $\mathbb{N}'^2$ using the expansion coefficients of $\varepsilon_r(\theta)$, i.e., c_m in (30),

Step 2: Construction of $\mathbb{P}_d$ and $\mathbb{P}_{\cos}$ with the help of Table 1,

Step 3: Construction of $\mathbb{H}_{\frac{1}{r^2}}$ and $\mathbb{H}_d$ with the help of Table 2,

Step 4: Calculation of the propagation constant and the complex amplitudes of TE_r and TM_r electromagnetic fields applying (35) and (37) or (36) and (38).

3. NUMERICAL RESULTS

To verify the proposed modal analysis, we have analyzed the configuration shown in Figure 3(a) in which a conical multilayer waveguide is terminated by two spherical conductors at R_1 and R_2 to form a resonator. In this example, the layers of the conical waveguide have a relative permittivity of $\varepsilon_{r_1} = 2.25$, $\varepsilon_{r_2} = 5.5$, $\varepsilon_{r_3} = 2.1$, and $\varepsilon_{r_4} = 3.78$ with the apex angles of $2\alpha_1 = 2\tan^{-1}\left(\frac{1}{2}\right)$, $2\alpha_2 = 2\tan^{-1}(1)$, $2\alpha_3 = 2\tan^{-1}\left(\frac{3}{2}\right)$, and $2\alpha_4 = 2\tan^{-1}(2)$, respectively. We have first determined the mode propagation constant k of the fundamental TM_r and TE_r modes of the conical waveguide by solving (35) and (36) for $M = N = 12$. Then, the mode propagation constant k is used to calculate the resonance frequency of the resonator shown in Figure 3(a). The resonance frequency is determined for various values of R_1 and R_2. This result is shown in the normalized form in Figure 3(b). The horizontal and vertical axes of this diagram are, respectively, $\frac{2\pi R_1}{\lambda_r}$ and $\frac{2\pi R_2}{\lambda_r}$ where λ_r is the wavelength at the resonance frequency. Conversely, for a given λ_r, every point of this diagram can be chosen as the working point from which the corresponding R_1 and R_2 are determined. To verify our results, the same resonator is also analyzed with the commercial software High Frequency Structure Simulator (HFSS) which is based on the method of finite element. The resonator has been analyzed for nine discrete values $(R_2 - R_1) = 5, 5.5, 6, 6.5, 7, 7.5, 8, 8.5\,\mathrm{mm}$ and 9 mm while R_1 has been kept constant at 10 mm. After the

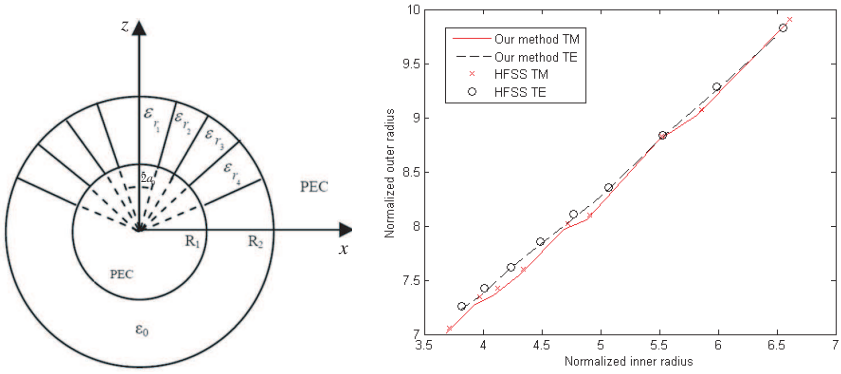

Figure 3. (a) A resonator compromised of a multilayer conical dielectric waveguide between two perfect conducting spheres. (b) Normalized resonance frequency of the first mode for $\varepsilon_{r_1} = 2.25$, $\varepsilon_{r_2} = 5.5$, $\varepsilon_{r_3} = 2.1$, and $\varepsilon_{r_4} = 3.78$ with the apex angles of $2\alpha_1 = 2\tan^{-1}\left(\frac{1}{2}\right)$, $2\alpha_2 = 2\tan^{-1}(1)$, $2\alpha_3 = 2\tan^{-1}\left(\frac{3}{2}\right)$, and $2\alpha_4 = 2\tan^{-1}(2)$. Solid line and dashed line represent our numerical results for TM_r and TE_r modes, respectively. Similarly, $\times$ and $\bullet$ show the results obtained using HFSS.

above mentioned normalization, the resonance frequencies calculated by HFSS for various $\frac{2\pi R_1}{\lambda_r}$ and $\frac{2\pi R_2}{\lambda_r}$ are also depicted in Figure 3(b). As can readily be seen in Figure 3(b), the HFSS results and those obtained using our modal analysis are in agreement. We should also mention that the computation of the mode propagation constant k for $M = 12$ and $N = 12$ required 0.18 seconds for each R_1 and R_2 while HFSS computation at this value of R_1 and R_2 with approximately 40,000 tetrahedra requires 320 seconds on the same PC. It must be mentioned that increasing M and N beyond 12 does not affect the value of the mode propagation constant k significantly.

As a second example, we have analyzed a biconical dielectric waveguide the configuration of which is shown in Figure 4(a). Each cone of this structure has a relative permittivity of $\varepsilon_r = 2.25$ and an apex angle of $2\alpha = 2\tan^{-1}\left(\frac{1}{2}\right)$. Here, the gray scale corresponds to magnitude of the E^θ for the first three TM_r modes. The borders of dielectric waveguide are specified by solid lines. Figure 4(b) shows the antenna mode of the biconical in which the distribution of the transverse electric field is mainly concentrated between the two dielectric cones. In the waveguide mode, the electric

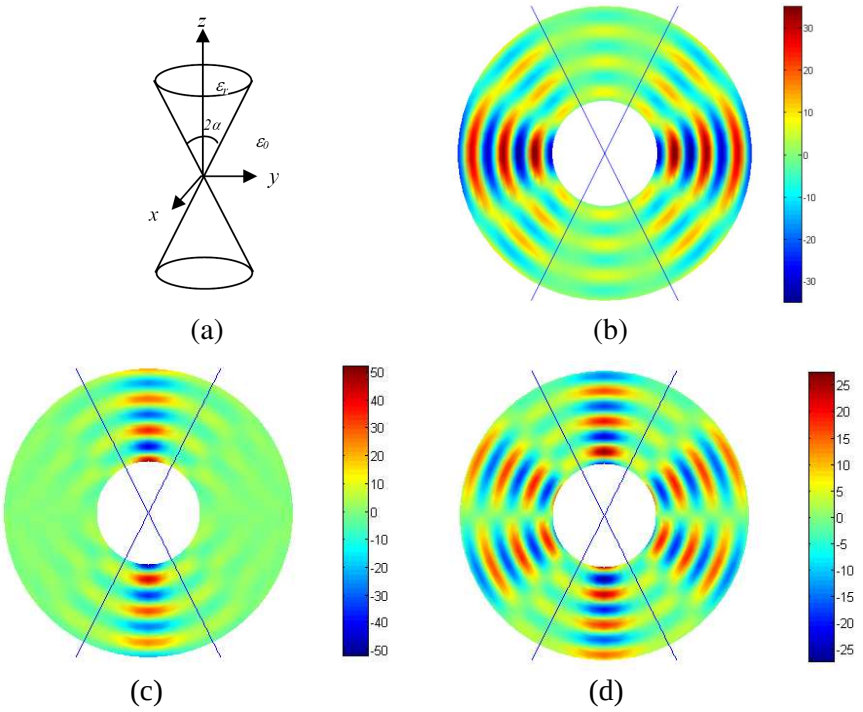

Figure 4. (a) A biconical dielectric waveguide constituted of $\varepsilon_r = 2.25$ with an apex angle of $2\alpha = 2\tan^{-1}\left(\frac{1}{2}\right)$ in free space. (b), (c), and (d) visualize the spatial distribution of E^{θ} for the first three TM_r modes in xz-plane.

field distribution concentrates in the dielectric cones as shown in Figure 4(c). Electromagnetic wave can propagate with a combination of antenna mode and waveguide mode, as shown in Figure 4(d).

4. CONCLUSION

We proposed a semi-analytical modal analysis for a multilayer conical dielectric waveguide after expanding the electric and magnetic fields on the basis of the Legendre polynomials and Schelkunoff functions. By applying a matrix representation of Maxwell's equations, we arrived at eigen-equations for the transverse (non-radial) components of the electromagnetic field and used their eigen-values and eigen-vectors to determine the propagation constant and the spatial distribution of various modes of a conical dielectric waveguide. Since there is no assumption on the values of dielectric constants in each layer of

conical waveguide, our numerical method can be used to analyze the structures with lossy dielectrics or the structures with negative dielectric constants such as plasmonic conical waveguides.

Verification of our numerical method has been done by calculating the resonance frequencies of resonators which are constituted of single layer dielectric waveguides. These results are in good agreement with those computed by HFSS. Because of its nature, our numerical method is by far faster than the FEM. A biconical dielectric waveguide has also been analyzed, and its modes are studied in detail.

REFERENCES

1. Sakai, J. I. and E. A. J. Marcatili, "Lossless dielectric tapers with three-dimensional geometry," *J. Lightw. Technol.*, Vol. 9, No. 3, 386–393, 1991.
2. Romanova, E. R., L. A. Melnikov, and E. V. Bekker, "Numerical analysis of total field propagation in linear and nonlinear singlemode tapered fibers," *International Conference on Transparent Optical Networks*, 161–164, 1999.
3. Paradasi, A., H. E. Hernandez-Figueroa, S. Celaschi, M. L. Brandao, T. Jesus, and M. Mercadante, "Beam propagation method modelling of optical filters based on tapered fibres," *IEEE Lasers and Electro-optics Society Annual Meeting, 1996. LEOS 96*, Vol. 2, 36–37, 1996.
4. Moar, P. N., S. T. Huntingtont, J. Katsifolis, L. W. Cahill, and K. A. N. Roberts, "A near field modelling and measurement of tapered optical fibre devices," *IEEE WG5*, 54–55, 1997.
5. Kawata, S., *Near-field Optics and Surface Plasmon Polaritons*, Springer, Berlin, 2001.
6. Srituravanich, W., N. Fang, C. Sun, Q. Luo, and X. Zhang, "Plasmonic nanolithography," *Nano Lett.*, Vol. 4, 1085, 2004.
7. Liu, Z. W., Q. G. Wei, and X. Zhang, "Surface plasmon interference nanolithography," *Nano Lett.*, Vol. 5, 957, 2005.
8. Kneipp, K., Y. Wang, H. Kneipp, L. T. Perelman, I. Itzkan, R. R. Dasari, and M. S. Feld, "Single molecule detection using surface-enhanced Raman scattering (SERS)," *Phys. Rev. Lett.*, Vol. 78, 1667, 1997.
9. Pettinger, B., B. Ren, G. Picardi, R. Schuster, and G. Ertl, "Nanoscale probing of adsorbed species by tip enhanced Raman spectroscopy," *Phys. Rev. Lett.*, Vol. 92, 096101, 2004.
10. Ichimaru, T., N. Hayazawa, M. Hashimoto, Y. Inouye, and S. Kawata, "Tip-enhanced coherent anti-Stokes Raman scattering

for vibrational nanoimaging," *Phys. Rev. Lett.*, Vol. 92, 220801, 2004.

11. De, A. and G. V. Attimarad, "Numerical analysis of two dimensional tapered dielectric waveguide," *Progress In Electromagnetics Research*, Vol. 44, 131–142, 2004.
12. Siong, C. C. and P. K. Choudhury, "Propagation characteristics of tapered core helical cald dielectric optical fibers," *Journal of Electromagnetic Waves and Applications*, Vol. 23, 663–674, 2009.
13. Jin, X., "Optical fiber index taper-theoretical analysis and experimental demonstration," *Int. J. Infrared Millimet. Waves*, Vol. 19, No. 6, 875–886, 1998.
14. Stockman, M. I., "Nanofocusing of optical energy in tapered plasmonic waveguides," *Phys. Rev. Lett.*, Vol. 93, 137404, 2004.
15. Taflove, A. and S. C. Hagness, *Computational Electrodynamics: The Finite Difference Time-domain Method*, 3rd edition, Norwood Artech House Publishers, 2005.
16. Khajehpour, A. and S. A. Mirtaheri, "Analysis of pyramid EM wave absorber by FDTD method and comparing with capacitance and homogenization methods," *Progress In Electromagnetics Research Letters*, Vol. 3, 123–131, 2008.
17. Kurihara, K., A. Otomo, A. Syouji, J. Takahara, K. Suzuki, and S. Yokoyama, "Superfocusing modes of surface plasmon polaritons in conical geometry based on the quasi-separation of variables approach," *J. Phys. A: Math. Theor.*, Vol. 40, 12479–12503, 2007.
18. Ruppin, R., "Scattering of electromagnetic radiation by a coated perfect electromagnetic conductor sphere," *Progress In Electromagnetics Research Letters*, Vol. 8, 53–62, 2009.
19. Issa, N. A. and R. Guckenberger, "Optical nanofocusing on tapered metallic waveguides," *Spr. Plas.*, Vol. 2, 31–37, 2007.
20. Harrington, R. F., *Time-harmonic Electromagnetic Fields*, IEEE Press Series on Electromagnetic Wave Theory, 2001.
21. Schelkunoff, S. A., *Electromagnetic Waves*, D. Van Nostrand Company, Inc. Princeton., N.J., 1943.
22. Lindell, I. V. and A. H. Sihvola, "Spherical resonator with db-boundary conditions," *Progress In Electromagnetics Research Letters*, Vol. 6, 131–137, 2009.
23. Adams, J. C., "On the expression of the product of any two Legendre's coefficients by means of a series of Legendre's coefficients," *Proc. R. Soc.*, Vol. 27, 63–71, 1878.